RSC Advances

ROYAL SOCIETY OF CHEMISTRY

www.rsc.org/advances

Can Si-embedded boron nitride nanotubes act as a favorable metal-free catalyst for CO oxidation by N_2O?

Mehdi D. Esrafili*, Nasibeh Saeidi, Parisa Nematollahi

Laboratory of Theoretical Chemistry, Department of Chemistry, University of Maragheh, Maragheh, Iran

* Corresponding author. **Phone:** (+98) 4212237955. **Fax:** (+98) 4212276060. **P.O. Box:** 5513864596. **E-mail**: esrafili@maragheh.ac.ir (Mehdi D. Esrafili).

Abstract

The oxidation of carbon monoxide (CO) as a toxic gas has a significant role in solving environmental problems and is important for a series of technological applications. In this paper, the oxidation of CO with N_2O molecule is studied over Si-doped (6,0) boron nitride nanotubes (Si-BNNTs) by means of density functional theory calculations. Also, reaction barriers and thermodynamic parameters are calculated using the M06-2X density functional with 6-31G* basis set. Si-doping of the BNNT at two possible substitution sites are explored, i.e. a boron site (Si_B) or a nitrogen site (Si_N). In both cases, the Si atom is found to be stabilized above the vacancy site after geometry relaxation. Also, the effects of increasing the tube length on the adsorption of gas molecules and CO oxidation reaction are studied in detail. Results show that the CO oxidation catalyzed by the Si-BNNTs is likely to occur at the room temperature. Besides, the Si_B substrate shows a better reactivity toward the CO oxidation due to its first barrier-less pathway and lower activation energy in second route (1.78 kcal/mol) than that in Si_N (9.75 kcal/mol).

Keywords: CO oxidation; N_2O reduction; Si-doping; BNNT; DFT.

1. Introduction

Nitrous oxide (N_2O) is known as a greenhouse gas which contributes to acid rain formation, photochemical smog and depletion of the ozone layer [1-3]. The main resource of this pollutant is the combustion of solid and liquid fuels especially at high temperatures [4]. Although today the N_2O gas is less abundant than methanol in the atmosphere, but it has a significant longer steady-state lifetime [5]. Therefore, it seems that the reduction of N_2O emission is an important topic for scientific investigations. Another poisonous gas which is produced from incompletely combustion of fossil fuels is carbon monoxide (CO). The oxidation of this toxic gas plays a significant role in solving the environmental problems caused by CO emission [6]. Therefore, according to recent studies [7,8] it is found that the oxidation of CO and reduction of N_2O gases become one of the major topics from the scientific view, in order to reduce these toxic pollutants. In the oxidation process, CO molecule can accept the oxygen atom which is transferred from the N_2O molecule. But, this process should have done over a favorable catalyst in order to provide a favorite path for this transmission. The activation energy of the direct reaction of N_2O with CO is so high which is hindered the reaction to take place at room temperature, therefore, the oxygen transfer reaction from N_2O to CO can be catalyzed by various transition metal cations in the gas phase [9]. According to recent experimental and theoretical investigations [10,11], there are two elementary reaction mechanisms for the oxygen transfer: first, the decomposition of N_2O over the catalyst which follows by the oxidation of CO as following equations:

$$N_2O \rightarrow N_2 + O^* \quad (1)$$

$$O^* + CO \rightarrow CO_2 \quad (2)$$

To date, many studies have been performed on the N_2O reduction by CO molecule which is catalyzed by transition metal cations [12-16]. For example, the landmark experiments of Kappes and Staley in 1981 demonstrated the first cyclic reduction of N_2O by CO in the gas phase in the presence of atomic metal cations [17]. Kartha et al [18] have found that the substituting Fe atom in lanthanum titanates enhances the catalytic activity for N_2O reduction by CO. Also, several studies on the CO oxidation reaction have been done over costly metal surfaces. Xu et al. [8] theoretically studied the reaction mechanisms for CO catalytic oxidation by N_2O or O_2 over the Co_3O_4 (110) surface. They found that N_2O or O_2 interacts with the oxygen vacancy site to regenerate the surface. The CO_2 molecule is formed when the activated O atom is attacked by the

second CO in a catalytic cycle. However, although there are many theoretical investigations on the reduction of N_2O by CO over different metal surfaces, but recently, scientists are tried to do this reaction over costless and favorable carbon-based materials with high activity for CO oxidation and N_2O reduction [19].

After the discovery of boron nitride nanotubes (BNNTs) in 1994 theoretically [20] and experimentally in 1995 [21], a great interest emerged for utilizing this amazing III-V nanostructures. BNNTs are structurally the same as carbon nanotubes (CNTs); they have monolith structures without dangling bonds on their surfaces and are strongest light-weight nanomaterials on earth which consist of co-axial hexagonal boron nitride (h-BN) networks [22]. Interestingly, BNNTs are semiconductors with a wide band gap independent of their helicity or tubular diameter [23]. In contrast to the covalent C–C bonds in CNTs, the B–N bonds in BNNTs have an ionic character due to the electronegativity difference between B and N atoms which make their dispersion in water much easier than nonionic CNTs [24]. In fact, in comparison with a limited number of experimental works, more papers were published theoretically about their electronic structures [24], property tuning [25], magnetic properties [26], hydrogen storage [27] and so on. Thus, due to the intrinsic properties of BNNTs, they can act as an outstanding sensor for detecting several gas pollutants such as CO, NO [28] and CO_2 [29]. Other related studies indicated that the properties of BNNTs increase at presence of impurities such as Si atom or introducing defects during their synthesis which enhances their sensing capability and solubility [30-33]. Zahng et al. [34] found that the Si-doped BNNTs have a strong chemical interaction with CO molecule while it has a weak physisorption over the pure BNNTs. As it is completely discussed in our previous work [35], when Si impurity is substituted at the site of B or N atom of the BNNT, the surface reactivity is increased significantly.

In this paper, Si-doping of BNNTs at two possible substitution sites are explored, i.e. a boron site (Si_B) or a nitrogen site (Si_N) by means of density functional theory (DFT) calculations. Also, CO oxidation mechanisms with N_2O molecule and its corresponding energy barriers are investigated in detail. To the best of our knowledge, no previous study has been reported for CO oxidation mechanism by N_2O over Si-embedded BNNTs (Si-BNNTs). Our results can be helpful for better understanding of the chemical properties of Si-BNNTs. It also has practical implications for the development of novel Si-BNNTs nanodevices such as gas sensors, metal-

free catalysts, and so on. In particular, these are very important for the development of an automobile catalytic converter that can clean up more than one gas by a single process.

2. Computational details

Full geometry optimization was performed at the M06-2X/6-31G* level of theory using the GAMESS suite of program [36]. M06-2X is a global-hybrid meta-GGA functional, with 54% Hartree-Fock exchange [37,38], which has been specifically designed to treat medium-range correlation energy, main group thermochemistry, non-covalent interactions and reaction barriers [39-41]. A truncated (6,0) BNNT with 30 B and 30 N atoms was chosen as the basic model for the calculations. Si-BNNTs were then modeled by substituting a single Si atom with one boron (Si_B) or nitrogen (Si_N) atom on BNNT (Figure 1). The unsaturated boundary effect was avoided by adding hydrogen atoms at the ends of BNNTs [42,43]. The corresponding frequency calculations were carried out at the same level in order to identify whether the optimized complexes correspond to a true local minimum or not. All transition state structures were characterized by frequency analysis and intrinsic reaction coordinate (IRC) calculations. Moreover, an elongated (6,0) BNNT with the length of about 13.64 Å was used to study the effect of increasing the length on the adsorption of gas molecules and CO oxidation reaction. The adsorption energy (E_{ads}) of gas molecules over Si-BNNTs is evaluated as follows:

$$E_{ads}(A) = E_{A-M} - E_M - E_A \quad (3)$$

where E_{A-M}, E_M and E_A are the total energies of the adsorbate-substrate (A–M) system, the substrate (M) and adsorbate (M), respectively. Natural bond orbital (NBO) [44] analysis was performed at the M06-2X/6-31G* level.

3. Results and discussions

3.1. Si-doping effect on geometric properties of the pristine BNNT

Figure 1 shows the optimized structures of pristine and Si-doped BNNTs at the M06-2X/6-31G* level of theory. For Si-doped BNNTs, one Si atom is located above the vacancy created at the site of B atom (Si_B) or nitrogen atom (Si_N). In both cases, the Si atom is found to be stabilized above the vacancy site after geometry optimization. One can see that the geometric structure of the BNNT is noticeably distorted when the Si atom is substituted at the site of B or N atom. The average B–N equilibrium distances in the pristine (6,0) BNNT is about 1.45 Å. Upon Si-doping, the Si dopant forms three strong covalent bonds with its nearest B/N atoms which make the Si–N and Si–B average bond lengths elongated to 1.75 Å and 1.99 Å in Si_B and Si_N,

respectively. These values are close to the corresponding bond lengths values of Si-doped (8,0) and (10.0) BNNTs [45,46]. Both increased bond lengths and different bond angles make Si atom to protrude outwardly from the nanotube surface, displacing also the positions of the neighboring atoms (see Figure 1). In both Si_B and Si_N structures, the Si atom shows a large adsorption energy (≈ -250 kcal/mol) at the vacancy site, because of the strong covalent bonds between the Si atom and nearest B/N atoms. Also, NBO analysis predicts a sizable electron transfer about 1.7 and 0.8 e from Si atom to the tube in Si_B and Si_N, respectively. This can stabilize the single Si atom and therefore increase the diffusion barrier of Si over the Si-BNNTs. These results confirm the fact that Si-BNNTs are stable enough to be utilized in catalytic CO oxidation by N_2O.

3.2. Adsorption of N_2O over the Si-BNNTs

Before exploring the CO oxidation by N_2O, the adsorption of N_2O and CO molecules over Si-BNNTs is individually studied in detail. It should be noted that for each adsorbate, various adsorption sites (including Si atom and its nearest B/N atoms) and different adsorption patterns (including side-on and end-on) are considered. The most favorable adsorption configurations of N_2O over Si-BNNTs are depicted in Figure 2 and the corresponding E_{ads} and thermodynamic parameters such as Gibbs free energy change (ΔG_{298}), enthalpy change (ΔH_{298}) and net charge transfer (q_{CT}) are listed in Table 1. According to the recent theoretical study [32], the N_2O molecule is attached to metal-embedded nanostructures with three typical possible configurations. First, it can be adsorbed from its O- or N-site in which the linear N_2O molecule is attached vertically to the active sites (metal-embedded or its neighboring atoms). Second and third are the N_2O adsorption via a [3+2]- and [2+2]-cycloaddition, respectively. Here, in the case of Si_B, the N_2O molecule is adsorbed via two stable configurations (**A** and **B**) (Figure 2). In the dissociative configuration (**A**), the N_2O molecule is easily decomposed to N_2 and O* species with corresponding N=N and Si-O* bond lengths of 1.10 and 1.68 Å, respectively, and with a noticeable adsorption energy (E_{ads}) of -78.49 kcal/mol. Of particular interest, the physisorbed N_2 molecule (Si-N = 3.18 Å) in this configuration is found to be easily released from the surface, leaving an O* atom attached to the Si atom of the tube. Also, there is about 0.3 e transfer from Si_B to the O* atom, which makes it more activated toward the adsorption of gas molecules. In order to investigate the electron density redistribution due to the adsorption of N_2O molecule over Si_B, electron density difference (EDD) plot is calculated, where the charge depletion and accumulation sites are displayed in yellow and blue, respectively. One can see a great charge

accumulation around the Si-O* bond, which confirms the chemical binding between the O* atom and surface. Additionally, according to thermochemistry results, the formation of configuration **A** is an exothermic process (ΔH_{298} = -78.41 kcal/mol), with a negative ΔG_{298} value of about -70.35 kcal/mol (Table 1).

Moreover, Figure 2 displays the molecular configuration **B**, with the E_{ads} of -27.16 kcal/more, in which the N_2O molecule is chemically adsorbed via its N atom with the Si atom of Si_B (Si-N = 1.79 Å). This adsorption leads to the great decrease in the N–N–O angle of N_2O from 180º in free N_2O to 137.84º in adsorbed form. Also, the corresponding N-N and N-O bond distances are increased from 1.12 and 1.18 Å in the gas molecule to 1.22 and 1.21 Å in **B**, respectively (Table 1). Similar to configuration **A**, from the NBO analysis, a net charge of 0.3 e is transferred from the Si_B to the N_2O molecule. Also, upon the N_2O adsorption, a considerable electron density is depleted from the vicinity of the Si atom and accumulated on the N_2O molecule. According to these results, which are consistent with the estimated chemisorptions energies, it can be suggested that the N_2O molecule tends to be adsorbed over Si_B via its dissociative configuration (**A**), due to its more negative E_{ads} and ΔG_{298} values (Figure 2, Table 1).

Continuously, the adsorption of N_2O molecule over Si_N is carefully studied. As Figure 2 indicates, the N_2O molecule can be attached to the Si atom of Si_N via its O or N atom and forms two different configurations named **C** and **D**. Interestingly, in both configurations, the N_2O molecule is adsorbed onto the Si_N in a [3 + 2]-cycloaddition and forms a five-membered ring. In the configuration **C**, in which N_2O attaches to the surface via its O atom, the formed Si_N-O, N-O, N-N and N-B bonds lengths are 1.69, 1.47, 1.19 and 1.54 Å, respectively (Figure 2). The E_{ads} of this configuration is about -28.34 kcal/mol while the negative values of ΔH_{298} and ΔG_{298} show that the formation of this complex is exothermic and is thermodynamically feasible (Table 1). In addition, a great charge of about 0.6 e transfers from the nanotube surface to the N_2O molecule and the blue regions in EDD isosurface confirm the formation of chemical binding between the N_2O and surface (see Figure 2).

On the other hand, in configuration **D**, the N_2O molecule is adsorbed via its N atom to the tube surface with a relatively smaller E_{ads} value (-19.78 kcal/mol) compared to the configuration **C**. The corresponding Si-N, N-N, N-O and B-O bond lengths are 1.78, 1.23, 1.34 and 1.49 Å, respectively (Figure 2). Comparing these values with those in configuration **C** shows that the smaller the O–N bond in Si–O–N=N, the more easily the formation of the N_2 gas. In contrast to

configuration **C**, despite the small absolute values of ΔH_{298} and ΔG_{298} (Table 1), the reaction is exothermic and can occur in an ambient temperatures. Also, similar to configuration **C,** about 0.6 e transfers from the surface to the N_2O molecule, which can be seen from its EDD map (Figure 2).

In summary, it can be concluded that among these four different adsorption configurations (**A** to **D**), the complexes in which the N_2O molecule adsorbs via its O atom over the Si atom of Si-BNNT (**A** and **C**) are the most energetically favorable configurations, due to their larger (more negative) E_{ads} and ΔG_{298} values. Furthermore, they are more favorable because in the former reactions, the O* atom is the most appropriate species to adsorb CO molecule and finally form and release the CO_2 gas from the tube surface.

After all, the effect of BNNT length on the adsorption of N_2O molecule is completely studied. To achieve the aim, first, Si-atom is individually substituted with B or N atom of the BNNT. The optimized structures of these Si-doped BNNTs are displayed in Figure S1 of Supporting Information. As it is clear, these structures have the almost same Si–N and Si–B bond lengths as those of short-length (6,0) BNNTs. It should be noted that after the adsorption of N_2O molecule, no structural changes are seen; therefore, they are named like before (Figure S2). Analogous with studied adsorbed configurations, the E_{ads} of complexes **B** and **D** are more than **A** and **C** structures (Table S1). It is found that there is not a significant difference between the N_2O adsorption over long-length and short-length (6,0) BNNTs. Hence, the size of the model considered for studying the adsorption of N_2O over the (6,0) BNNT is validated.

3.3. Adsorption of CO over the Si-BNNTs

In order to find the most stable configuration of a single CO molecule adsorbed on the Si-BNNTs, different possible adsorption configurations are considered. The most stable configurations of CO adsorption over Si-BNNTs in which the CO molecule is adsorbed via its C atom over the Si atom of the surface are displayed in Figure 2. Also, the E_{ads}, ΔH_{298}, ΔG_{298} and q_{CT} are summarized in Table 1. The end-on adsorption configuration is found to be the most energetically preferred structure in which CO molecule is adsorbed over the Si atom of the tube surface. The estimated E_{ads} values of the CO-Si_B and CO-Si_N complexes are about -4.3 and -3.6 kcal/mol, respectively. This shows that the former system is the preferred structure for the adsorption of a CO molecule over Si-BNNTs. Also, there is a shorter binding distance between the end-on CO molecule and the Si_B (1.93 Å) compared to Si_N (1.98 Å) which is another reason for choosing the CO-Si_B as the most suitable system for CO adsorption. There are about 0.15

(0.13) e charge transfer from the Si_B (Si_N) to the $2\pi^*$ orbital of CO molecule which leads to the C-O bond elongation from 1.13 Å in free CO molecule to 1.18 (1.17 Å) in the adsorbed Si_B (Si_N) configurations (Figure 2). It is also evident from the EDD map that there is a small charge density accumulation around the CO molecule and Si atom of Si-BNNTs. This indicates that CO is a weaker electron acceptor than the N_2O molecule. According to these results, it can be concluded that the CO adsorption with its weaker E_{ads} and smaller q_{CT} values, has less effect on the Si-BNNTs surface. So, it may be estimated that if a CO/N_2O mixture is injected as a reaction gas, the Si atom of Si-BNNT should be dominantly covered by adsorbed N_2O molecules.

Considering the effect of tube length on the adsorption properties of CO molecule shows that the corresponding binding distance and adsorption energy have no significant changes in comparison with those on short-length (6,0) BNNT. It is clear from Figure S3 and relative values in Table S1 that analogous with the CO adsorption configurations on short-length (6,0) BNNT, the CO molecule has a negligible effect on the electronic structure properties of the long-length tube due to its lower E_{ads} magnitudes. Therefore, at presence of N_2O/CO molecules, the tube prefers to be covered with N_2O molecule rather than CO.

3.4. Reaction pathways of CO oxidation by N_2O

In order to investigate the reaction mechanisms of the CO oxidation by N_2O molecule over the Si-BNNTs, we start from the most favorable configurations (**A** and **C**) due to the formation of the activated atomic oxygen (O*). Figure 3 shows the possible reaction pathways of CO oxidation over both configurations **A** and **C**. Also, the configurations of the initial state (IS), transition state (TS) and final state (FS) with their related geometric parameters are demonstrated in Figure 4. The corresponding activation energy (E_{act}) as well as thermodynamic parameters such as ΔH_{298} and ΔG_{298} of the elementary reaction pathways are listed in Table 2. As mentioned before, in the configuration **A**, the N_2O molecule is dissociated to the N_2 and atomic O* species. In fact, during the formation of **A** complex, the reaction pathway of **A** $\rightarrow$ Si_B-O* + N_2 occurs automatically, passing through a negligible activation energy. Moreover, in the next pathway, Si_B-O* + CO $\rightarrow$ CO_2, the possibility of using the atomic O* for CO oxidation reaction in complex **A** is studied in detail. According to above discussion, dissociative configuration **A** is chosen as the FS-1 due to the physisorption of N_2 molecule with the tube (Si-N_2 = 3.18 Å and N-N_2 = 3.49 Å). After desorption of N_2 gas, several distinct coadsorbed Si_B-O* + CO

configurations are examined in order to find and select the most appropriate structure to form the stable configuration Si_B-O* + CO. Among them, the complex in which the CO molecule is 2.68 Å far from the atomic O* is chosen as the IS (Figure 4). It is found that the CO molecule reaches and reacts by with the atomic O* with an energy barrier of 1.78 kcal/mol. This energy barrier is fairly lower than those of noble metal catalysts such as Au-doped graphene [47] or those using normal transition metals, such as Fe [48] and Cu [49]. In the transition state (TS-1), the distance of O*-C is reduced to 2.04 Å. Passing through TS-1, the final product (Si_B + CO_2) is achieved where the CO_2 molecule places in parallel position with tube surface and is physically adsorbed over the Si atom of the surface. Also, according to Table 2, this reaction is exothermic with ΔH_{298} value of -13.27 kcal/mol. It should be mentioned that the formed CO_2 molecule has a weak interaction with the tube surface and therefore it can easily desorbs from the reactive site at room temperature and makes the catalyst renewed.

On the other hand, in configuration **C**, N_2 and atomic O* species are formed passing through the transition state TS-2, with a small activation energy of 0.04 kcal/mol. This E_{act} is smaller than that reported on Ru- (9.4 kcal/mol) [50] and Pt-embedded graphene (23.7 kcal/mol) [51]. Because of this small E_{act} value, it is expected that decomposition of N_2O over the Si_N can be achieved quite easily. In TS-2, a five-membered ring is formed over Si_N in which the Si-O and O-N bond lengths are decreased and increased to 1.67 and 1.53 Å, respectively. Passing over TS-2, the distance of Si-O is continuously contracted from 1.67 to 1.57 Å until Si_N-O* + N_2 is achieved. In this state, the formed N_2 with the N=N bond, which is reduced from 1.19 in TS-2 to 1.01 Å in the Si_N-O* + N_2 state, and N–Si (N–B) distance of 3.31 (2.75 Å), desorbs from the surface while the activated O* atom remains on the tube surface with B-N_2 binding distance of 2.75 Å. In the next step, Si_N-O* + CO → CO_2, the possibility of using the atomic O* for the CO oxidation reaction in configurations **C** is investigated. After approaching the CO molecule to the atomic O*, different coadsorbed Si_N-O* + CO configurations are obtained. The reaction starts with the most favorable Si_N-O* + CO configuration in which the CO molecule is placed about 2.99 Å far from the atomic O* (Figure 4) with the E_{act} of 9.75 kcal/mol. Besides, in the complex **C**, the Si_N-O* bond distance (1.57 Å) is slightly shorter than Si_B-O* (1.68 Å) in **A**, therefore, it can be estimated that the extra energy is needed for the removal of atomic O* from the reaction Si_N substrate. It is important to know that in the CO oxidation over Si_N, the Si_N-O* + CO → Si_N + CO_2 reaction can be considered as the rate limiting step. In TS-3, the distance of O*–C is

reduced to 1.91 Å. Passing through TS-3, the Si_N + CO_2 is achieved where the CO_2 molecule places in parallel position with tube surface and physically adsorbs with the Si atom of the surface. According to Table 2, the reaction pathway of Si_N-O* + CO → Si_N + CO_2 is exothermic with ΔH_{298} value of -22.70 kcal/mol. Also, the formed CO_2 has a weak interaction with the tube surface which leads to its desorption at an ambient conditions.

To better understand the tube length effect on the CO oxidation mechanism with N_2O molecule, all of the studied mechanisms were also considered over the long-length (6,0) Si-BNNTs. It is noteworthy that the obtained results are in close agreement with those obtained in short-length (6,0) BNNT. The local configurations of IS, TS and FS along with their geometric values are displayed in Figure S3. Pathway **A** → Si_B-O* + N_2 is barrier-less while Si_B-O* + CO → CO_2 proceeds via the E_{act} of 2.35 kcal/mol. In Si_N-BNNT, the estimated barrier energy for **C** → Si_N-O* + N_2 and Si_N-O* + CO → CO_2 reactions are calculated to be 0.05 and 9.69 kcal/mol, respectively. It is clear that similar with previous pathways, the E_{act} of these reaction routs don't significantly change. Thus, it can be concluded that the oxidation reaction of CO by N_2O molecule has a negligible dependency on the length of the BNNT.

In short, it is found that Si-BNNTs have an outstanding catalytic activity toward the CO oxidation. It can be concluded from the obtained activation barriers that Si_N substrate has a greater E_{act} than that of Si_B in the O* + CO → CO_2 reaction pathway. Also, in comparison with Si_N, the corresponding oxidation reaction of dissociative configuration **A** can take place rapidly at room temperature because of its barrier-less **A** → Si_B-O* + N_2 reaction pathway. Therefore, unlike Si_N, the Si_B substrate shows a better reactivity toward the CO oxidation due to its first barrier-less pathway and lower E_{act} in second route (1.78 kcal/mol) than that in Si_N (9.75 kcal/mol). These results can be helpful for developing effective metal-free catalysts for the oxidation of CO based on BNNTs.

4. Conclusion

In summary, the catalytic oxidation of CO and reduction of N_2O molecule over the Si-BNNTs is studied by means of DFT calculations. Results indicate that Si-BNNTs can stabilize the single Si atom and increase its diffusion barrier. Comparing the E_{ads} values of CO and N_2O molecules over Si-BNNTs show that the CO molecule has a weaker ability as an electron acceptor than the N_2O molecule. These results suggest that when a mixture of N_2O and CO molecules is injected as the reaction gas, the Si atom of Si-BNNTs should be covered by N_2O

molecule. In the configuration **A**, the barrierless reaction pathway **A** → Si_B-O* + N_2 occurs rapidly at room temperature in which the N_2 molecule and atomic O* species are formed. Due to the far distance of N_2 molecule with the tube surface, it can easily desorbs from the Si_B surface and makes the Si_B-O* activated for the second pathway: Si_B-O* + CO → CO_2. The E_{act} of this step (1.78 kcal/mol) is considerably lower than that in Si_N substrate (9.75 kcal/mol), so, it can be estimated that Si_B has a better catalytic activity than Si_N for CO oxidation with N_2O molecule. Our results reveal that the length of BNNT has a negligible influence on the oxidation reaction of CO by N_2O molecule. It can be suggested that Si-BNNTs may be considered as a capable candidate for low-temperature CO oxidation reaction by N_2O molecule with lower cost and higher activity.

References

[1] R. A. Duce, J. LaRoche, K. Altieri, K. R. Arrigo, A. R. Baker, D. G. Capone, S. Cornell, F. Dentener, J. Galloway, R. S. Ganeshram, R. J. Geider, T. Jickells, M. M. Kuypers, R. Langlois, P. S. Liss, S. M. Liu, J. J. Middelburg, C. M. Moore, S. Nickovic, A. Oschlies, T. Pedersen, J. Prospero, R. Schlitzer, S. Seitzinger, L. L. Sorensen, M. Uematsu, O. Ulloa, M. Voss, B. Ward and L. Zamora, *Science,* 2008, **320**, 893.

[2] A. R. Ravishankara, J. S. Daniel and R. W. Portmann, *Science,* 2009, **326**, 123.

[3] S. A. Montzka, E. J. Dlugokencky and J. H. Butler, *Nature,* 2011, **476**, 43.

[4] T. Rockmann, J. Kaiser and C. A. M. Brenninkmeijer, *Atmos. Chem. Phys. Discuss.,* 2002, **2**, 2021.

[5] J. Hsu and M. J. Prather, *Geophys. Res. Lett.,* 2010, **37**, L07805.

[6] S. Royer and D. Duprez, *ChemCatChem,* 2011, **3**, 24.

[7] H. J. Freund, G. Meijer, M. Scheffler, R. Schlögl and M. Wolf, *Angew. Chem. Int. Ed.,* 2011, **50** 10064.

[8] X. L. Xu, E. Yang, J. Q. Li, Y. Li and W. K. Chen, *ChemCatChem,* 2009, **1**, 384.

[9] H. Loirat, F. Caralp, M. Destriau and R. Lesclaux, *J. Phys. Chem.,* 1987, **91**, 6538.

[10] F. Rondinelli, N. Russo and M. Toscano, *J. Chem. Theory Comput.,* 2008, **4**, 1886.

[11] L. Zhao, Z. Liu, W. Guo, L. Zhang, F. Zhang, H. Zhu and H. Shan, *Phys. Chem. Chem. Phys.,* 2009, **11**, 4219.

[12] A. Trovarelli, *Catal. Rev.-Sci. Eng.,* 1996, **38**, 439.

[13] A. Eichler, *Surf. Sci.,* 2002, **498**, 314.

[14] P. Salo, K. Honkala, M. Alatalo and K. Laasonen, *Surf. Sci.,* 2002, **516**, 247.

[15] M.S. Chen, Y. Cai, Z. Yan, K.K. Gath, S. Axnanda and D. Wayne Goodman, *Surf. Sci.,* 2007, **601**, 5326.

[16] Y. Lin, Z. Wu, J. Wen, K. Ding, X. Yang, K.R. Poeppelmeier and L. D. Marks, *Nano Lett.,* 2015, **15**, 5375.

[17] M. M. Kappes and R. H. Staley, *J. Am. Chem. Soc.,* 1981, **103**, 1286.

[18] K. K. Kartha, M. R. Pai, A. M. Banerjee, R. V. Pai, S. S. Meena and S. R. Bharadwaj, *J. Mol. Catal. A: Chem.,* 2011, **335**, 158.

[19] S. Wannakao, T. Nongnual, P. Khongpracha, T. Maihom and J. Limtrakul, *J. Phys. Chem. C,* 2012, **116**, 16992.

[20] A. Rubio, J. L. Corkill and M. L. Cohen, *Phys. Rev. B,* 1994, **49**, 5081.

[21] N. G. Chopra, R. J. Luyken, K. Cherrey, V. H. Crespi, M. L. Cohen, S. G. Louie and A. Zettl, *Science,* 1995, **269**, 966.

[22] J. Wang, V. K. Kayastha, Y. K. Yap, Z. Fan, J. G. Lu, Z. Pan, I. N. Ivanov and A. A. Puretzky, *Nano Lett.,* 2005, **5**, 2528.

[23] X. Blase, A. Rubio, A. G. Louie and M. L. Cohen, *Euro. Phys. Lett.,* 1994, **28**, 335.

[24] D. Golberg, Y. Bando, Y. Huang, T. Terao, M. Mitome, C. Tang and C. Zhi, *ACS Nano* 2010, **4**, 2979.

[25] K. H. Khoo, M. S. C. Mazzoni and S. G. Louie, *Phys. Rev. B* 2004, **69**, 201401.

[26] R. Q. Wu, L. Liu, G. W. Peng and Y. P. Feng, *Appl. Phys. Lett.,* 2005, **86**, 122510.

[27] G. Mpourmpakis and G. E. Froudakis, *Catal. Today,* 2007, **120**, 341.

[28] Y. Xie, Y. Huo and J. Zhang, *Appl. Surf. Sci.,* 2012, **258**, 6391.

[29] H. Choi, Y. Ch. Park, Y. H. Kim and Y. S. Lee, *J. Am. Chem. Soc.,* 2011, **133**, 2084.

[30] Y. Chen, X. C. Yang, Y. J. Liu, J. X. Zhao, Q. H. Cai and X. Z. Wang, *J. Mol. Graph. Model.,* 2013, **39**, 126.

[31] Y. Chen, B. Gao, J. X. Zhao, Q. H. Cai and H. G. Fu, *J. Mol. Model.,* 2012, **18**, 2043.

[32] J. X. Zhao, Y. Chen and H. G. Fu, *Theor. Chem. Acc.,* 2012, **131**, 1242.

[33] Y. J. Cho, C. H. Kim, H. S. Kim, J. Park, H. Ch. Choi, H. J. Shin, G. Gao and H. S. Kang, *Chem. Mater.,* 2009, **21**, 136.

[34] R. Wang and D. Zhang, *Aust. J. Chem.,* 2008, **61**, 941.

[35] M. D. Esrafili, *Struct. Chem.,* 2013, **24**, 1207.

[36] M. W. Schmidt, K. K. Baldridge, J. A. Boatz, S. T. Elbert, M. S. Gordon, J. H. Jensen, S. Koseki, N. Matsunaga, K. A. Nguyen, S. J. Su, T. L. Windus, M. Dupuis and J. A. Montgomery, *J. Comput. Chem.,* 1993, **14**, 1347.

[37] Y. Zhao, N. E. Schultz and D. G. Truhlar, *J. Chem. Phys.,* 2005, **123**, 161103.

[38] Y. Zhao and D. G. Truhlar, *Acc. Chem. Res.,* 2008, **41**, 157.

[39] K. Yang, R. Peverati, D.G. Truhlar and R. Valero, *J. Chem. Phys.,* 2005, **135**, 044118.

[40] Y. Zhao and D.G. Truhlar, *J. Am. Chem. Soc.,* 2007, **129**, 8440.

[41] M.D. Esrafili and R. Nurazar, *Comput. Mater. Sci.,* 2014, **92**, 172.

[42] G. Zhou, W. Duan and B. Gu, *Phys. Rev. Lett.,* 2001, **87**, 095504.

[43] C. W. Chen and M. H. Lee, *Nanotechnology,* 2004, **15**, 480.

[44] A. E. Reed, L. A. Curtiss and F. Weinhold, *Chem. Rev.,* 1988, **88**, 899.

[45] S. Guerini, T. Kar and P. Piquini, *Eur. Phys. J. B,* 2004, **38**, 515.

[46] R.Wang, R. Zhu and D. Zhang, *Chem. Phys. Lett.,* 2008, **467**, 131.

[47] Y. H. Lu, M. Zhou, C. Zhang and Y. P. Feng, *J. Phys. Chem. C,* 2009, **113**, 20156.

[48] Y. F. Li, Z. Zhou, G. T. Yu, W. Chen and Z. F. Chen, *J. Phys. Chem. C,* 2010, **114**, 6250.

[49] E. H. Song, Z. Wen and Q. Jiang, *J. Phys. Chem. C,* 2011,**115**, 3678.

[50] C. Huang, X. Ye, C. Chen, S. Lin and D. Xie, *Comput. Theor. Chem.*, 2013, **1011**, 5.

[51] Y. Tang, Z. Yang and X. Dai, *Phys. Chem. Chem. Phys.,* 2012, **14**, 16566.

Table 1. Calculated binding distances (R), net charge-transfer (q_{CT}), adsorption energy (E_{ads}), change of Gibbs free energy (ΔG_{298}) and change of enthalpy (ΔH_{298}) for the adsorption of N_2O and CO over Si_B and Si_N substrates

surface	R (Å)	q_{CT} (e)	E_{ads} (kcal/mol)	ΔG_{298} (kcal/mol)	ΔH_{298} (kcal/mol)
N_2O-Si_B					
A	1.68	0.32	-78.49	-70.35	-78.41
B	1.79	0.29	-27.16	-15.22	-26.23
N_2O-Si_N					
C	1.69	0.63	-28.34	-16.41	-28.30
D	1.78	0.60	-19.78	-7.25	-20.24
CO-Si_B	1.93	0.15	-4.30	-3.11	-4.23
CO-Si_N	1.98	0.13	-3.60	-2.83	-3.55

Table 2. Calculated activation energy (E_{act}), reaction energy (ΔE), change of Gibbs free energy (ΔG_{298}) and change of enthalpy (ΔH_{298}) for different pathways of CO oxidation by N_2O molecule over Si_B and Si_N substrates

Reaction	E_{act} (kcal/mol)	ΔE (kcal/mol)	ΔG_{298} (kcal/mol)	ΔH_{298} (kcal/mol)
Si_B-BNNT				
A → Si_B-O* + N_2	-	-	-70.35	-78.41
Si_B-O* + CO → CO_2	1.78	-13.27	-12.20	-13.27
Si_N-BNNT				
C → Si_N-O* + N_2	0.04	-40.96	-46.59	-40.96
Si_N-O* + CO → CO_2	9.75	-22.70	-21.00	-22.70

Figure 1. Optimized structure and bond lengths (in Å) of pristine and Si-BNNTs. Color code for each optimized structure: blue ball: N; pink ball: B; light gray ball: Si.

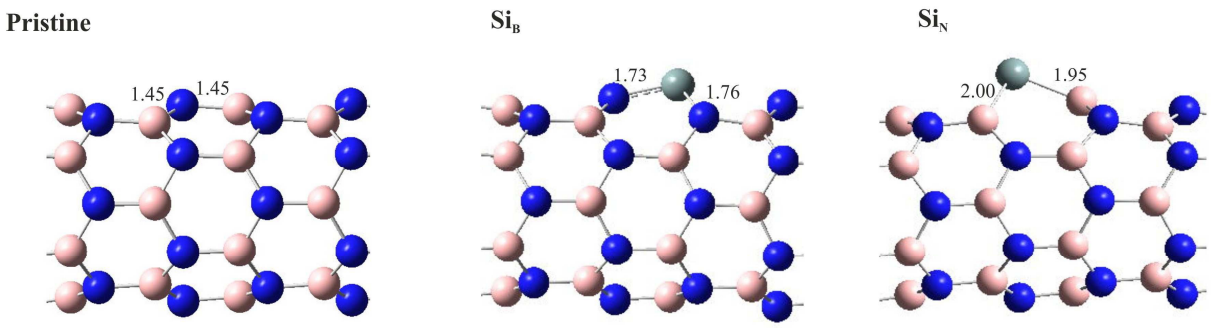

Figure 2. Optimized structures and electron density difference plots for N_2O and CO adsorption over Si-BNNTs. All distances are in Å. In the electron density difference plots charge depletion and accumulation are displayed in yellow and blue, respectively. Color code for each optimized structure: blue ball: N; pink ball: B; red ball: O; light gray ball: Si; dark gray ball: C.

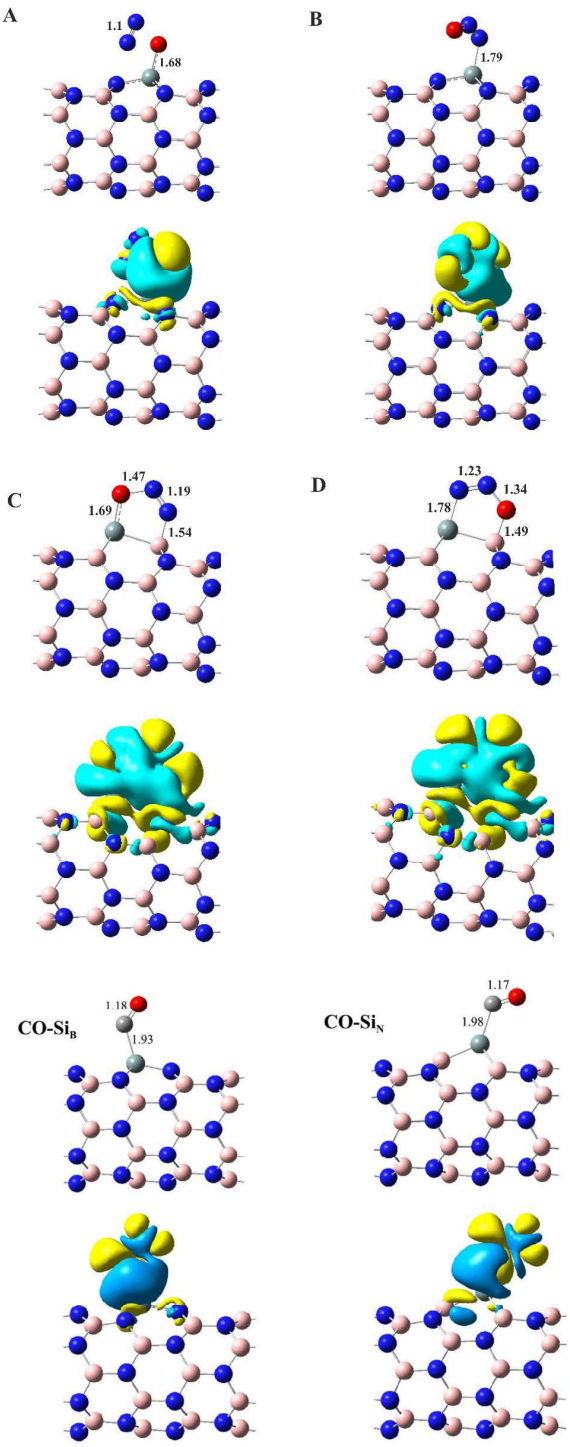

Figure 3. Reaction energy profiles for oxidation of CO by N_2O over Si-BNNTs. All energy values are in kcal/mol.

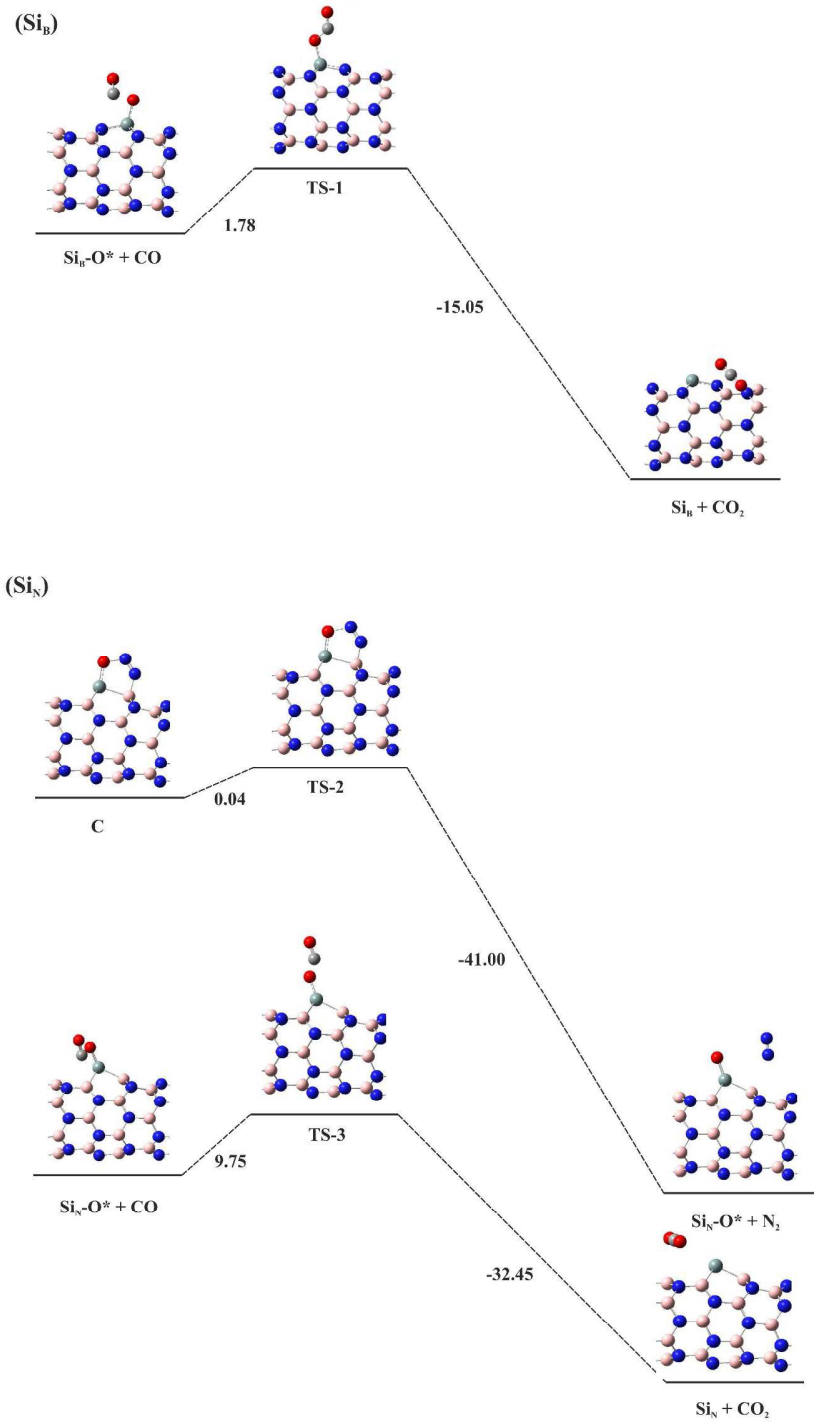

Figure 4. Optimized structures of stationary points for different reaction pathways. All distances are in Å.

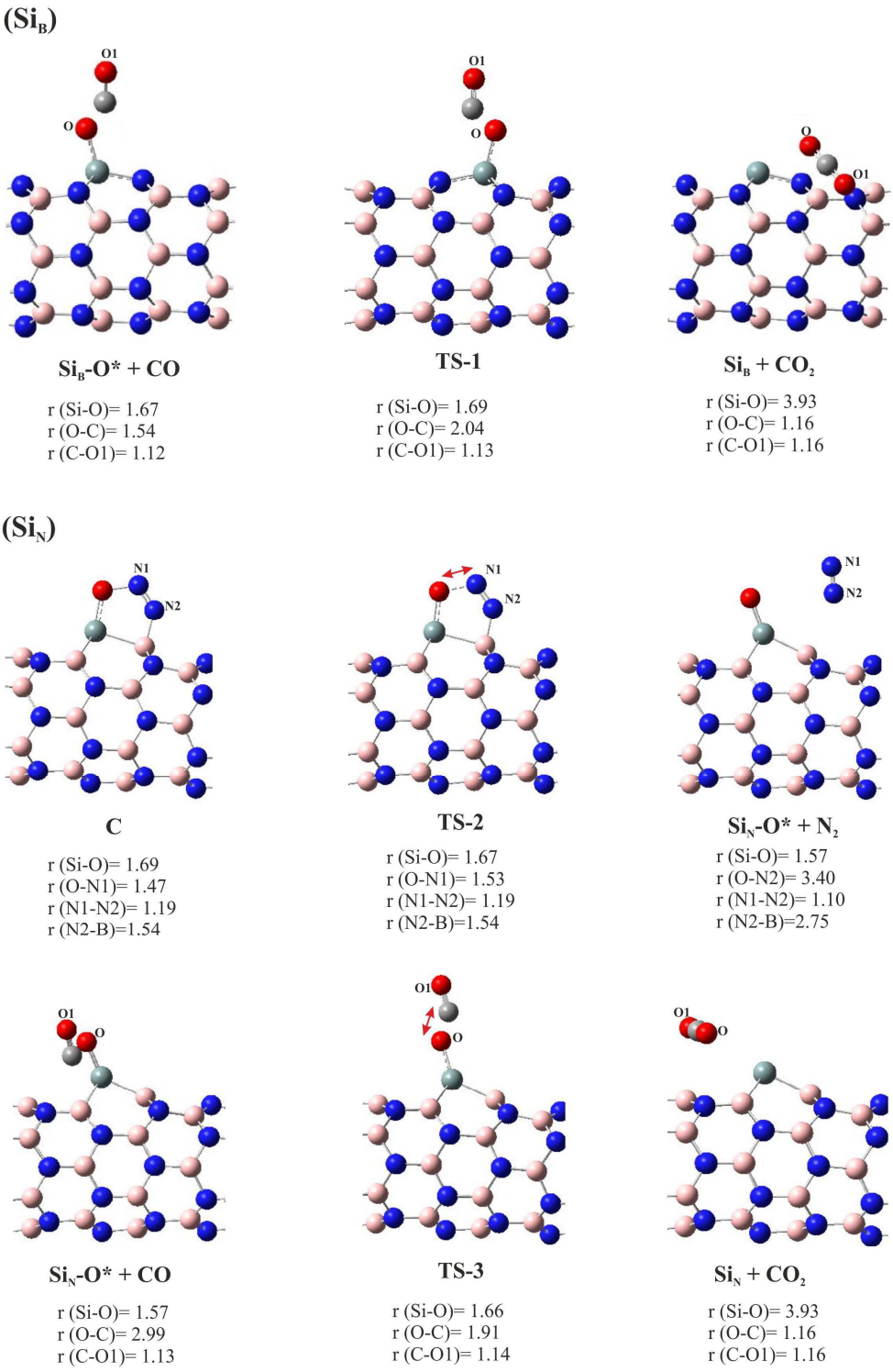

Graphical abstract

N_2O adsorption over Si-doped BNNT